Icarus 216 (2011) 111–115

Contents lists available at SciVerse ScienceDirect

Icarus

journal homepage: www.elsevier.com/locate/icarus

Note

Carbon dioxide glaciers on Mars: Products of recent low obliquity epochs (?)

Mikhail A. Kreslavsky [a,*], James W. Head [b]

[a] Earth and Planetary Sciences, University of California – Santa Cruz, 1156 High Street, Santa Cruz, CA 95064, USA

[b] Department of Geological Sciences, Brown University, Box 1846, Providence, RI 02912, USA

ARTICLE INFO

Article history:
Received 17 January 2011
Revised 15 August 2011
Accepted 24 August 2011
Available online 1 September 2011

Keywords:
Mars, Polar geology
Mars, Climate
Ices

ABSTRACT

Three localized sets of small arcuate ridges associated with slopes in the northern polar area of Mars (~70°N latitude) are morphologically similar to sets of drop moraines left by episodes of advance and retreat of cold-based glaciers. Comparison with other glacial features on Mars shows that these features differ in important aspects from those associated with water–ice flow. Instead, we interpret these features to be due to perennial accumulation and flow of solid carbon dioxide during recent periods of very low spin-axis obliquity.

1. Introduction

Water ice is known to be abundant on the surface and in the shallow subsurface on Mars, especially (but not exclusively) at high and middle latitudes. On Earth, the most common ice morphologies are ice sheets and alpine glaciers, both intrinsically related to dynamic water ice accumulation, ablation and flow. At first glance, Mars lacks such active features, which is a logical consequence of the currently extremely cold (unfavorable for ice flow) and hyperarid (unfavorable for dynamic accumulation) climate conditions. Detailed studies, however, have revealed abundant morphologies suggestive of ice flow in the past. Three different types of ice flow morphologies have been identified on Mars: (1) small (hundreds of m long, tens of m thick) lobes at the steepest slopes in mid-latitudes dubbed as viscous flow features (VFF) (e.g., Milliken et al., 2003); (2) lobate debris aprons (LDA), lineated valley fill, and concentric crater fill, mid-latitude features genetically similar to each other that are from a km of spatial extent to 100s of km long, 100s of m thick and arguably thicker in the past (e.g., Head et al., 2010; Baker et al., 2010), and (3) deposits from tropical mountain glaciers (TMG), features of hundreds of km in spatial extent with inferred ice thickness of a few km during the epochs when they were active (e.g., Head and Marchant, 2003; Shean et al., 2005). Not surprisingly, the most applicable terrestrial morphological analogs for martian water ice flow features are cold-based glaciers (deforming internally, without basal melting and basal sliding) found in the coldest terrestrial environments (Marchant et al., 1993).

Here we report on an additional type of distinctive cold-based glacial morphology on Mars that we refer as high-latitude glaciers, HLG. They are represented by small ridges forming narrow overlapping loops. One occurrence has been found and described in detail by Garvin et al. (2006); another one has been discussed by Kreslavsky and Head (2007). Here we show that the FLG are hard to explain by the flow of water (H_2O) ice; instead, we suggest that they were formed by carbon dioxide (CO_2) glaciers.

2. Occurrence and morphology

We systematically searched for evidence of narrow elongated lobes on all large steep slopes at northern high latitudes (from 55°N to the edge of the main part of the polar layered deposit; PLD) using THEMIS daytime IR images. Our search in southern hemisphere high latitudes was also extensive but revealed no additional similar features. We found or confirmed a total of three locations with narrow arch-like ridges, all at high northern latitudes. The most extensive set (Kreslavsky and Head, 2007) occurs at 74°N, 96°E (Fig. 1) in association with the northwest-facing steep slopes of a PLD outlier. The ridges are distinctive and arch-like (in planform view), forming more than 40 parallel and overlapping loops over a distance of about 110 km; these are grouped in three sets with gaps between them. The individual ridges are 15–80 m wide, are generally continuous, and show little width and height variation along strike. The loops formed by these ridges are most typically 5–7 km in long axis, and ~1.5–10 km wide. In several cases, the ridges are superposed on old heavily modified impact craters and/or on the extended deposits surrounding them; no evidence of modification of the underlying deposits or structures is observed in association with the ridges and related deposits; these relationships all suggest a geologically youthful age. HiRISE images (e.g., PSP_009717_2545) show that the ridges are mantled and covered with the typical high-latitude polygonal pattern almost uniformly with their surroundings. Some of the ridges, and thus the loops, are superposed on one another. In the middle group (Fig. 1b) a generally continuous ridge set extends distally for a distance of up to 15 km (arrow in Fig. 1b); the ridge is subdued in some places along its strike. Shorter loops contained within this deposit are clearly superposed on this larger ridge complex occurrence. The proximal parts of the looped ridges are open toward the steep wall of the PLD outlier and are separated from it by a 10 to 20 km wide gap.

A second set of narrow ridges with lobate planform occur inside a 26.8 km-diameter crater located at 70.3°N, 266.5°E (Fig. 2a) (Garvin et al., 2006). Ridges here are somewhat wider (100–200 m wide) and the lobes extend up to 15–20 km from the south-eastern wall of the crater. At least 5 subsets of overlapping ridges are distinguishable. Newly acquired images show that the lobes are open to the east, that the eastern ends of the ridges are at the lower part of the crater wall, and no special morphology is observed on the wall itself. In addition, a few arcuate concentric ridges occur at the outer, eastern slope of the crater rim (Fig. 2a). HiRISE images (e.g., PSP_009803_2505) show that here too the ridges are superposed by typical polygonal patterns almost uniformly blending with their surroundings.

A third set of similar ridges (not previously documented) occurs inside a 24 km crater at 67.2°N, 249.5°E (Fig. 2b). In this example, three to five overlapping lobes extend westward from the eastern wall over the crater floor, in a manner similar to the previous example. Here the outermost ridge is best preserved; it forms a 4–5 km wide lobe that extends ~14 km from the crater wall. In a manner similar

* Corresponding author.
E-mail address: mkreslav@ucsc.edu (M.A. Kreslavsky).

0019-1035/$ - see front matter © 2011 Published by Elsevier Inc.
doi:10.1016/j.icarus.2011.08.020

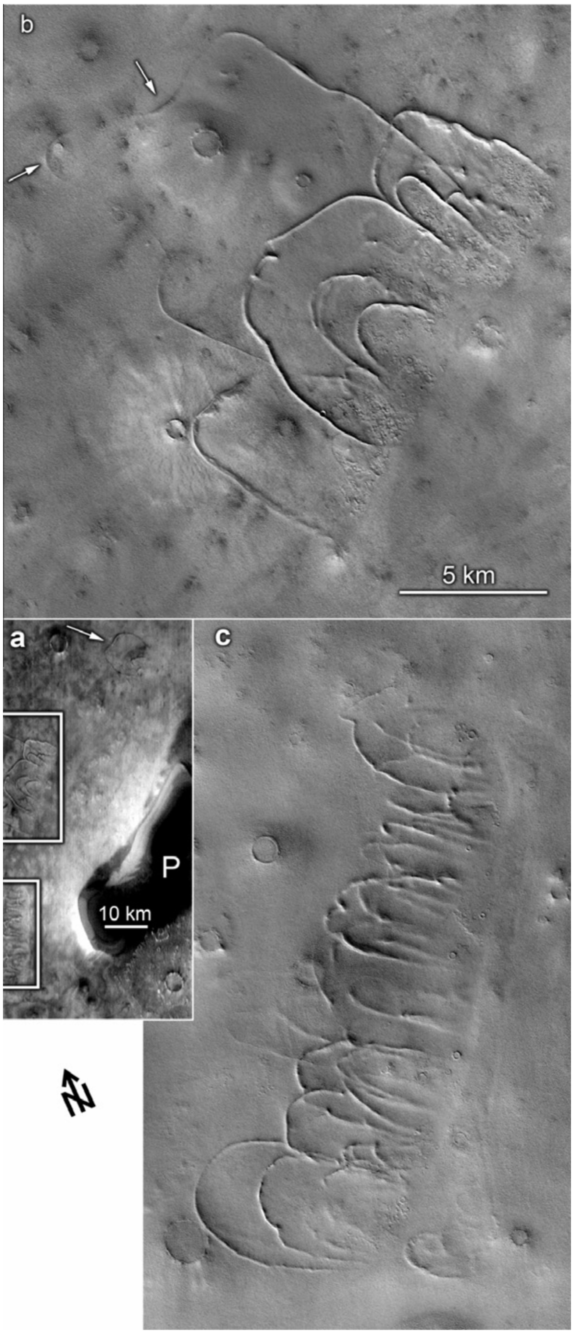

Fig. 1. High-latitude glacier (HLG) deposits at 74°N96°E. (a) part of THEMIS daytime thermal IR image I11693002. The PLD outlier (P) is black (cold); arrow shows the northern group of ridges, and the frames outline the middle and the southern groups shown in b and c. (b), middle and (c), southern group of features from CTX image P16_007357_2541. The scene in this image is covered with seasonal frost, and contrasting albedo markings do not mask topography. Arrows in (b) show the most extended loop.

to the previous occurrence, this ridge is 100–200 m wide, and two narrower ridges form concentric arcs on the outer, eastern slope of the crater rim.

3. Interpretation

On the basis of detailed considerations, Garvin et al. (2006) showed that the looped ridges in Fig. 2a are very similar to ridges typical of drop moraines in terrestrial cold-based glacial environments (see Fig. 12b in Garvin et al. (2006)). Drop moraines form when cold-based glaciers advance and then dynamically stabilize (the ice advance is balanced by frontal ice ablation); in this case, debris carried forward by the glacier drops out at the glacial front as sublimation of the ice occurs and a drop moraine is produced (e.g., Marchant et al., 1993; Marchant and Head, 2007). Overlapping ridges form due to multiple episodes of glacier advance and retreat. The strong morphological similarity of all three occurrences allows us to extend this interpretation to all considered features that we refer as high-latitude glaciers, HLG. The gap between the PLD outlier wall and the HLG (Fig. 1) is interpreted to have formed by later retreat of the PLD outlier due to sublimation; such a retreat is plausible because the PLD material is known to be H_2O ice with an unknown proportion of dust, and is known to be able to sublimate and retreat.

The total area outlined by the outermost lobate ridges in all three HLG locations is about 1000 km^2. Accurate inference about the thickness of the glacier, when it was active, is impossible, however, its order of magnitude can be reliably constrained. In the crater in Fig. 2a the glacier flow is obviously deflected by the central peak of the crater (which is ~400 m high), but one of the lobes climbed almost to its summit; this is only possible if during this episode of glacier advance, the glacier thickness between the crater wall and the peak was greater than ~400 m. Similarly, the westernmost tip of the ridge loop in the crater in Fig. 2b is ~200 m above the lowermost central part of the crater. On the other hand, the craters are 1.3 km and 1.2 km deep (rim crest to floor), and it is difficult to imagine that a flow thicker than a kilometer would be so strongly controlled by crater topography. Thus, several hundred meters is a reliable order-of-magnitude estimate of the flow thickness in the craters. The PLD outlier is currently about 100 m high; perhaps, it was taller before retreat, however it have never been thicker than a typical PLD thickness of 1–2 km, that is comparable or somewhat lower than the crater walls. The strong morphological similarity between the outlier-associated lobes and the lobes in the craters suggests a similar thickness of the flowing material. Assuming several hundred meters thickness for the whole area outlined with the lobate ridges, we obtain a total volume of glacier material on the order of several hundreds of km^3, or a few mm of global equivalent layer over the entire planet. The time scale of formation of these features (duration of advance, stabilization and retreat forming a single lobe) is poorly constrained. Quasi-periodic oscillations of spin axis obliquity with a period about 110 ka (Laskar et al., 2004) cause strong variations of the insolation pattern in polar regions and hence drive strong climate changes. It is probable that each episode of stable moraine-forming glacial flow was not longer than the characteristic time scale of stability of the obliquity-forced climate, a few tens of ka.

A characteristic basal shear stress for a body of ice on a horizontal substrate is scaled as $\sim\frac{1}{2}\rho g H^2/L$, where ρ is ice density, g is gravity, H and L are characteristic vertical and horizontal dimensions. For the horizontal (a few km) and vertical (several hundred m) dimensions discussed above, the shear stress is bracketed between 10^4 and 10^5 Pa. We now compare these stress and flow geometry with other glacial features on Mars, VFF, LDA, and TMG.

The mid-latitude lobate features, VFF, interpreted as flow of icy material (e.g., Milliken et al., 2003) have thicknesses of ~10 m and more; their morphology suggests that they were thicker (~100 m) when active. They are limited to steep slopes and never extend far on horizontal surfaces; it is quite probable that the total strain in these flows is on the order of unity or less. In contrast, the HLG can flow up to 15 km away from the slope; apparently, the total strain exceeds unity by an order of magnitude or more. The basal shear stress of the VFF is $\sim 10^4$ Pa (assuming the present-day thickness of ~10 m) to $\sim 10^5$ Pa (assuming the inferred thickness of ~100 m), comparable to the HLG, while the total strain is significantly less. The difference in time scales of glacier formation hardly can account for the observed difference in the total strain: the obliquity cycle limits the maximum duration of each single episode of VFF activity at the midlatitudes in the same way as for the HLG in the polar areas. On the other hand, it is difficult to imagine that the VFF were formed at much shorter times scales (100s of years); consideration of ice rheology by Milliken et al. (2003) clearly suggest longer time scales. Thus, the high total strain indicates that the material of the HLG is weaker than the material of the VFF. Morphology suggests that the VFF still contain at least some ice remaining from the times where the glacier-like flow was active, while the material formed the HLG does not exist anymore and only moraines are left.

Other types of flow features observed at the midlatitudes of Mars are lobate debris aprons (LDA), lineated valley fill, and concentric crater fill (see review by Carr and Head (2010) and references therein), features that possibly are genetically similar. Of these, lobate debris aprons are of special interest for our comparison, because these features are formed in similar topographic settings, on rather flat surfaces in association with steep slopes; smaller LDA have the same thickness and spatial extent (e.g., Li et al., 2005) as the HLG, hence, the inferred basal shear stress is similar. However, their morphology is very different. Although the LDA are indeed somewhat lobate, the HLG have much more lobate planforms, forming rather narrow lobes in similar topographic settings (Fig. 1), which suggests some difference in rheology. In addition, a significant part of the original icy material is still preserved in the LDA, as it is suggested by morphology (e.g., Li et al., 2005; Baker et al., 2010) and observed by radar (Holt et al., 2008; Plaut et al., 2009). Shallow ground ice is expected to be stable throughout the obliquity cycle at the HLG locations (e.g., Mellon and Jakosky, 1995), but it is unstable now and expected to be unstable through a significant part of the obliquity cycle at midlatitudes, where the LDS are located. Thus, all other circumstances being the same, we would expect better preservation of ice at high latitude in comparison to the lobate debris aprons; a special explanation is needed for simultaneous preservation of ice at lower latitude and its removal at high latitudes. A difference in the composition of the flow material is one possible explanation; an abundance of debris forming a protective lag at the surface is an alternative possibility.

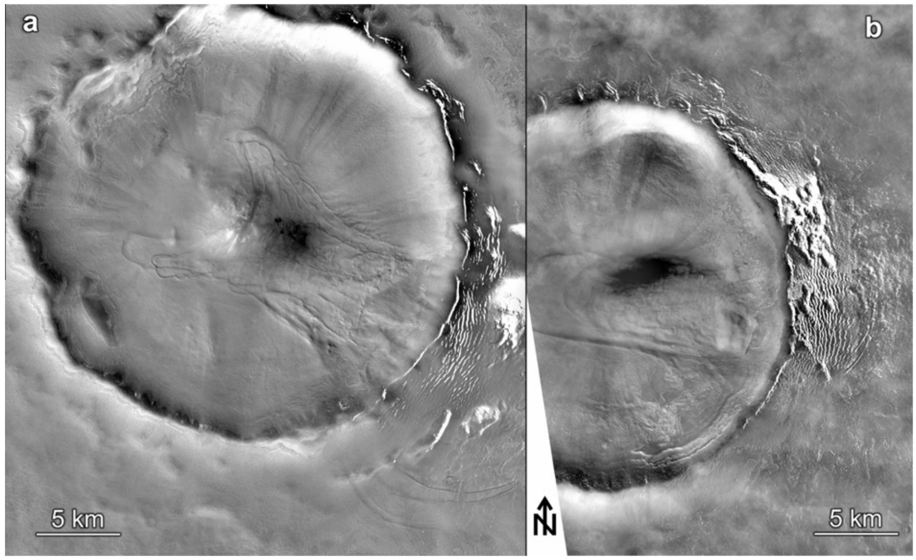

Fig. 2. (a) HLG in a crater at 70.3°N, 266.5°E from CTX image T01_000876_2505. (b) HLG in a crater at 67.2°N249.5°E from CTX image P18_008182_2474.

The tropical mountain glacier deposits on Mars (TMG) display ridges also interpreted as drop moraines left by cold-based glaciers (e.g., Head and Marchant, 2003; Shean et al., 2005). The TMG are much larger (e.g., 0.17×10^6 km^2 on Arsia Mons) and imply an original ice thickness on the order of a few km (Shean et al., 2005; Fastook et al., 2008); a thickness of 2 km and a typical slope of 0.3° imply a basal shear stress of 3×10^4 Pa, comparable to the HLG. In the TMG the moraines are distributed in very broad arches along the margins of the deposit and are mostly regularly concentric rather than overlapping and lobate, which again suggest some difference in rheology. The typical time scale of formation of tropical mountain glaciers is a Ma or longer (Fastook et al., 2008) and exceeds a single obliquity cycle, however, individual moraines were likely formed within a single obliquity cycle, and the time scale for accumulation of significant strain is the same as for HLG.

Finally, one more possible object for comparison is the PLD, which has basal shear stress on the order of 10^4 Pa, comparable or slightly lower than for the HLG. Although some authors interpret the general shape of a part of the PLD as evidence for ice flow in the past (e.g., Winebrenner et al., 2008), morphological evidence (e.g., Tanaka et al., 2008) and radar-derived internal configuration of layers (Holt et al., 2010) are not consistent with flow, while the age of the main stack of layers is almost certainly older than a few Ma. The observed absence of flow in the PLD at Ma time scale again suggests that H_2O ice, the PLD material, is much stiffer than the material of the HLG.

How do we account for the unusual weakness of the HLG material in comparison to VFF, LDA, and PLD? Ice plasticity is strongly controlled by temperature. The year-average surface temperature (which is approximately equal to the temperature inside the glacier) is lower at high latitudes than in the tropics and mid-latitudes, unless the spin-axis obliquity is extremely high ($\gtrsim 60°$). The obliquity of Mars can be accurately traced back in time to ~20 Ma (Laskar et al., 2004) (Fig. 3); the high-latitude glaciers are almost certainly younger than 20 Ma, and hence they were formed when obliquity never exceeded 48°. Thus, it is impossible

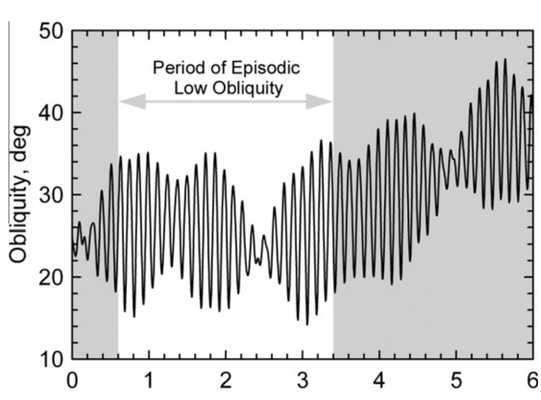

Fig. 3. Evolution of obliquity for the last 6 Ma with the epoch of episodic low obliquity from 3.4 to 0.6 Ma ago marked.

to explain the high plasticity of the HLG material with high temperature. The PLD does not flow under similar temperature, and the VFF, LDA, and TMG formed under higher temperatures in comparison to the HLG. Although basal shear stresses and flow time scales for HLG and TMG are comparable, TMG flow under significantly higher temperatures; this means that under the same temperature the HLG material would be significantly weaker than the TMG material. We conclude that difference in materials comprising the glaciers is the cause of the observed unusual rheology of these features, and that the material that flowed and formed drop moraines of HLG is not water ice. We suggest that dry ice, solid carbon dioxide (CO_2), is a plausible candidate for such material; dry ice is known to be much softer than H_2O ice at the same temperature (e.g., Durham et al., 1999; Nye et al., 2000). Although the confining lithostatic pressure at the base of a few hundred meter thick slab of CO_2 is above the CO_2 triple point, the expected basal temperatures of the HLG are below the melting point (~217 K), and the CO_2 glacier would be cold-based, in accordance with the observations.

The flow law of solid CO_2 measured by Durham et al. (1999) is directly applicable to our consideration, because those experiments were carried out under temperatures, confining pressures, and strain rates relevant to our case. This flow law was approximated in a traditionally used power-law relation between shear stress σ and strain rate $\dot{\varepsilon}$:

$$\dot{\varepsilon} = A(T)\sigma^n, \quad (1)$$

where stress exponent n and temperature-dependent stiffness coefficient $A(T)$ are fit parameters. If we consider a 400 m thick uniform slab of solid CO_2 on 20° steep slope under temperature of 145 K (the present-atmosphere frost point), the flow law from (Durham et al., 1999) yields a flow velocity of ~4 m per year, just enough to produce kilometers-long lobes during a few thousands of years. The CO_2 flow law is highly non-linear with the stress exponent of $n \sim 6$, hence, just a little "better" conditions immediately lead to very fast flow. The lower layers of the CO_2 glacier were certainly warmer than the frost point, because the glacier was deposited on a surface with a higher long-term-average temperature (the present-day year-average temperature there is about 165 K). If we increase the temperature to 160 K and the slab thickness to 600 m, the velocity will dramatically increase to ~1 km per year. These order-of-magnitude estimates show that solid CO_2 is soft enough to produce flows of the observed dimensions at a thousand-year time scale.

The high stress exponent of the CO_2 flow law ($n \sim 6$) in comparison to H_2O ice flow ($n \sim 3$) is consistent with more lobate planforms of CO_2 glaciers. The stronger non-linearity makes dry ice flow quickly, when flow starts. This leads to spatial concentration of strain and hence to spontaneous formation of lobes. This phenomenon is well known for two-dimensional viscous fingering (e.g., Homsy, 1987). Although in the case of viscous fingering the configuration of flow is different, the physical mechanism of increased lobateness for non-linear rheology is the same as we envision for glacial flow. Spectacular examples of increase of lobateness of viscous fingers caused by increased non-linearity have been obtained in laboratory experiments by Yamamoto et al. (2001) (see their Figs. 3a, 4a, and 5a), and in numerical simulations by Yamamoto et al. (2002) (see their Fig. 8). Thus, the difference in the stress exponent between CO_2 and H_2O ices is consistent with the observed higher lobateness of the HLG in comparison to the LDA and TMG.

Another argument for a non-H_2O nature of the flowing material is association of the flows with a wall of the PLD outlier (Fig. 1). The outlier material itself has regular horizontal layering and does not show any lobate morphology suggestive of flow. Ice cannot flow on a stable slope made of the same ice. Flowing of weaker water ice on top of thick stiff water ice is difficult to imagine. The shear stress, σ, driving the glacier flow is approximately proportional to the depth from the surface. Thus, in the flow law (1), σ^n at the base of the body of ice is an order of magnitude higher then somewhere in the middle (because $n \sim 3$). Strain rate, $\dot{\varepsilon}$, at the base can be negligibly small in comparison to that in the middle only if stiffness, $A(T)$, of the lower layer is at least two orders of magnitude higher than in the upper flowing layer. Structural differences (for example, different grain sizes and/or different concentrations of dust) cannot account for such big difference in stiffness, but temperature can. A noticeable temperature inversion (warmer softer ice on top of colder stiffer ice) can in principle be created by intensive accumulation of warmer ice after an abrupt climate change; however, this would require annual ice accumulation exceeding the annual thermal skin depth, that is a few meters of net ice accumulation each year, which seems unrealistic for Mars. In summary, we conclude that flow over water ice does require ice of different composition.

We have previously predicted glaciers composed of solid carbon dioxide on Mars (Kreslavsky and Head, 2005): it has long been understood that at low obliquity the atmospheric CO_2 condenses to make perennial deposits, and we showed that they are thickest at steep pole-facing slopes at high latitudes. The upper limit of ice volume estimated above corresponds to $\sim 2 \times 10^{-5}$ of the present-day atmosphere of Mars, a tiny part of all CO_2 that should have condensed into perennial deposits during each low-obliquity period. Recently discovered massive CO_2 deposits in the upper layers of the southern PLD (Phillips et al., 2011) show that accumulation of solid CO_2 indeed occurred on Mars in the recent past, as well as that the total amount of CO_2 available for condensation at low obliquity could be almost twice larger than now.

Solid CO_2 accumulation at low obliquity is predicted to be favored on north-facing slopes (Kreslavsky and Head, 2005). The HLG are associated with west- and north-west-facing slopes. Since CO_2 is the dominant component of the present-day atmosphere, its accumulation is controlled primarily by direct heat balance, unlike solid H_2O accumulation on the Earth, where microenvironments may take control. The observed slope orientation can be explained in two ways that do not exclude each other. First, the HLG could form when a significant part of the present-day atmosphere was in perennial deposits of dry ice (on horizontal surfaces, hence not flowing and leaving no record); the relative abundance of nitrogen and argon in the atmosphere was high, and CO_2 did not behave as the dominant atmospheric component. Second, photochemical models of the atmosphere under a wide range of conditions (Zahnle et al., 2008) show that if H_2O abundance in the atmosphere is significantly lower than the present, CO_2 is partly replaced by oxygen O_2 and carbon monoxide CO (both gases never condense on Mars). At low obliquity, the H_2O vapor abundance is expected to be very low (all H_2O vapor is trapped in the perennially cold solid CO_2 deposits), and CO_2 may lose its dominance in the atmospheric composition, which would allow accumulation on west-facing slopes.

We also considered (Kreslavsky and Head, 2007) another possible flowing glacier material on Mars, sulfur dioxide (SO_2); transient SO_2 in the atmosphere could result form massive volcanism. While solid SO_2 could play a role in much earlier parts of the martian geological record, it is very improbable (and unsupported by observations) that massive volcanic events capable of supplying a significant amount of sulfur occurred within the last few Ma, as suggested by the moraine ages. Ages of the latest massive volcanism obtained from crater counts exceed 20–50 Ma (e.g., Werner, 2009). The photochemical lifetime of SO_2 in the present-day or similar climate conditions is too short (e.g., Wong et al., 2004) for glacier formation. Thus, we prefer a CO_2 ice explanation for these features.

The material that flowed in the HLG no longer exists. Moraines left by the flow are comprised of different material than the material that flowed. The debris in terrestrial H_2O glaciers that produces the moraine material is generally talus derived from cliffs above the glacier accumulation area and entrained into ice flow, or is deposited from the atmosphere. For glaciers flowing on the slope of the PLD outlier, no source of talus is available. The moraine material could consist of dust co-deposited as condensation nuclei or as eolian dust. It might also contain H_2O ice deposited as frost or snow on the CO_2 glacier.

Calculation of the spin and orbit evolution of Mars (Laskar et al., 2004) shows that the obliquity was low (<18°) for a few short periods between 3.4 and 0.6 Ma ago (Fig. 3), and had not been low at least for a few tens of Ma before that period. This provides a rather certain age estimate of 0.6–0.8 Ma for the youngest HLG. The oldest HLG may be as old as 3.4 Ma, but also could be $\sim$1.0 Ma old. The individual low-obliquity periods are short (a few ka), and it appears plausible that a single episode of glacier advance and retreat (hence, one drop-moraine loop) could correspond to a single obliquity minimum. On the basis of the fact that the oldest moraine loops are largest, and there were at least 4–5 episodes of CO_2 glaciation, it appears more plausible that the oldest (the most extensive) HLG is $\sim$2 Ma or $\sim$3 Ma old (see Fig. 3). Not every obliquity minimum may lead to CO_2 glacier formation: an appropriate combination of eccentricity and season of perihelion, in addition to low obliquity, may be needed for intensive accumulation of CO_2 in certain microenvironments.

4. Further implications

The identification of CO_2 glaciers on Mars is not only interesting in itself, but it has significant consequences for understanding recent climate-controlled processes in the martian arctic, in particular, processes of evolution of patterned ground, the terrain surrounding the Phoenix landing site, and the PLD. The fact that the polygonal cracks are superposed over the moraines uniformly with the surroundings indicates that the observed polygonal cracks are younger than 0.6–0.8 Ma. On the other hand, the fact that the moraines are clearly visible and rather sharp indicates that the total modification of the surface during the last 1–2 Ma was relatively minor, although consistent with deposition of meter-thick mantles and/or meter-scale deflation due to sublimation (Head et al., 2003).

Association of the moraines with the PLD outlier indicates that the outlier existed at least 0.6 Ma ago and perhaps, 1–2 Ma ago, while the area to the west of it was free of PLD material. The western wall of the outlier remained at almost the same position during the epoch of obliquity oscillations from 1 or 2 Ma to 0.6 Ma ago and retreated by 10–20 km during the last 0.6 Ma. This gives an independent estimate of the time scales of evolution of the PLD walls and troughs.

Acknowledgments

Discussions with Kevin Zahnle and Oded Aharonson were very helpful. Reviews by Kenneth Tanaka, Asmin Pathare and an anonymous reviewer helped to improve the paper. This work was partly supported by NASA awards NNX08AN09G, NNX08AL07G, NNG05GQ46G, and NNX07AN95G.

References

Baker, D.M.H., Head, J.W., Marchant, D.R., 2010. Flow patterns of lobate debris aprons and lineated valley fill north of Ismeniae Fossae, Mars: Evidence for extensive mid-latitude glaciation in the Late Amazonian. Icarus 207, 186–209.

Carr, M.H., Head, J.W., 2010. Geologic history of Mars. Earth Planet. Sci. Lett. 294, 185–203.

Durham, W.B., Kirby, S.H., Stern, L.A., 1999. Steady-state flow of solid CO_2: Preliminary results. Geophys. Res. Lett. 26, 3493–3496.

Fastook, J.L., Head, J.W., Marchant, D.R., Forget, F., 2008. Tropical mountain glaciers on Mars: Altitude-dependence of ice accumulation, accumulation conditions, formation times, glacier dynamics, and implications for planetary spin-axis/orbital history. Icarus 198, 305–317.

Garvin, J.B., Head, J.W., Marchant, D.R., Kreslavsky, M.A., 2006. High-latitude cold-based glacial deposits on Mars: Multiple superposed drop moraines in a crater interior at 70°N latitude. Meteorit. Planet. Sci. 41, 1659–1674.

Head, J.W., Marchant, D.R., 2003. Cold-based mountain glaciers on Mars: Western Arsia Mons. Geology 31, 641–644.

Head, J.W., Mustard, J.F., Kreslavsky, M.A., Milliken, R.E., Marchant, D.R., 2003. Recent ice ages on Mars. Nature 426, 797–802.

Head, J.W., Marchant, D.R., Dickson, J.L., Kress, A., Baker, D.M., 2010. Northern mid-latitude glaciation in the Late Amazonian period of Mars: Criteria for the recognition of debris-covered glacier and valley glacier landsystem deposits. Earth Planet. Sci. Lett. 294, 306–320.

Holt, J.W. et al., 2008. Radar sounding evidence for buried glaciers in the southern mid-latitudes of Mars. Science 322, 1235–1238.

Holt, J.W. et al., 2010. The construction of Chasma Boreale on Mars. Nature 465, 446–449.

Homsy, G.M., 1987. Viscous fingering in porous media. Ann. Rev. Fluid Mech. 19, 271–311.

Kreslavsky, M.A., Head, J.W., 2005. Mars at very low obliquity: Atmospheric collapse and the fate of volatiles. Geophys. Res. Lett. 32, L12202.

Kreslavsky, M.A., Head, J.W., 2007. Unusual glacial-like features in the high-arctic of Mars. Lunar Planet. Sci. XXXVIII, 1576 (abstract).

Laskar, J., Correia, A.C.M., Gastineau, M., Joutel, F., Levrard, B., Robutel, P., 2004. Long term evolution and chaotic diffusion of the insolation quantities of Mars. Icarus 170, 343–364.

Li, H., Robinson, M.S., Jurdy, D.M., 2005. Origin of martian northern hemisphere mid-latitude lobate debris aprons. Icarus 176, 382–394.

Marchant, D.R., Head, J.W., 2007. Antarctic dry valleys: Microclimate zonation, variable geomorphic processes, and implications for assessing climate change on Mars. Icarus 192, 187–222.

Marchant, D.R., Denton, G.H., Sugden, D.E., Swisher, C.C., 1993. Miocene glacial stratigraphy and landscape evolution of the western Asgard Range, Antarctica. Geografiska Annaler 75A, 303–330.

Mellon, M.T., Jakosky, B.M., 1995. The distribution and behavior of martian ground ice during past and present epochs. J. Geophys. Res. 100, 11781–11799.

Milliken, R.E., Mustard, J.F., Goldsby, D.L., 2003. Viscous flow features on the surface of Mars: Observations from high-resolution Mars Orbiter Camera (MOC) images. J. Geophys. Res. 108. doi:10.1029/2002JE002005.

Nye, J.F., Durham, W.B., Schenk, P.M., Moore, J.M., 2000. The instability of a south polar cap on mars composed of carbon dioxide. Icarus 144, 449–455.

Phillips, R.J. et al., 2011. Massive CO_2 ice deposits sequestered in the south polar layered deposits of Mars. Science 332, 838–841.

Plaut, J.J. et al., 2009. Radar evidence for ice in lobate debris aprons in the mid-northern latitudes of Mars. Geophys. Res. Lett. 36, L02203.

Shean, D.E., Head, J.W., Marchant, D.R., 2005. Origin and evolution of a cold-based tropical mountain glacier on Mars: The Pavonis Mons fan-shaped deposit. J. Geophys. Res. 110, E05001.

Tanaka, K.L., Rodriguez, J., Alexis, P., Skinner, J.A., Bourke, M.C., Fortezzo, C.M., Herkenhoff, K.E., Kolb, E.J., Okubo, C.H., 2008. North polar region of Mars: Advances in stratigraphy, structure, and erosional modification. Icarus 196, 318–358.

Werner, S.C., 2009. The global martian volcanic evolutionary history. Icarus 201, 44–68.
Winebrenner, D.P., Koutnik, M.R., Waddington, E.D., Pathare, A.V., Murray, B.C., Byrne, S., Bamber, J.L., 2008. Evidence for ice flow prior to trough formation in the martian north polar layered deposits. Icarus 195, 90–105.
Wong, A.S., Atreya, S.K., Formisano, V., Encrenaz, T., Ignatiev, N.I., 2004. Atmospheric photochemistry above possible martian hot spots. Adv. Space Res. 33, 2236–2239.
Yamamoto, T., Kamikawa, H., Tanaka, H., Nakamura, K., Mori, N., 2001. Viscous fingering of non-newtonian fluids in a rectangular Hele-Shaw cell. J. Soc. Rheol. Jpn. (Nihon Reoroji Gakkaishi) 29, 81–87.
Yamamoto, T., Kamikawa, H., Mori, N., Nakamura, K., 2002. Numerical Simulation of viscous fingering of non-newtonian fluids in a Hele-Shaw cell. J. Soc. Rheol. Jpn. (Nihon Reoroji Gakkaishi) 30, 121–127.
Zahnle, K., Haberle, R.M., Catling, D.C., Kasting, J.F., 2008. Photochemical instability of the ancient martian atmosphere. J. Geophys. Res. 113, E11004.